Nonlocal Euler-Bernoulli beam theories with material nonlinearity and their application to single-walled carbon nanotubes

kun huang (kunhuang2008@163.com)
Kunming University of Science and Technology https://orcid.org/0000-0001-5194-1255
Benning Qu
Kunming University of Science and Technology
Wei Xu
Kunming University of Science and Technology
Ji Yao
Kunming University of Science and Technology

Research Article

Keywords: Euler-Bernoulli beam theory, Nonlocal elasticity, Material nonlinearity, Single-walled carbon nanotubes, Softening effect

Posted Date: March 1st, 2022

DOI: https://doi.org/10.21203/rs.3.rs-847357/v3

Abstract

Although the small-scale effect and the material nonlinearity significantly impact the mechanical properties of nanobeams, their combined effects have not attracted researchers' attention. In the present paper, we propose two new nonlinear nonlocal Euler-Bernoulli theories to model nanobeam's mechanical properties corresponding to extensible or inextensible locus. Two new theories consider the material nonlinearity and the small-scale effect induced by the nonlocal effect. The new models are used to analyze the static bending and the forced vibration for single-walled carbon nanotubes (SWCNTs). The results indicate that the material nonlinearity and the nonlocal effect significantly impact SWCNT's mechanical properties. Therefore, neglecting the two factors may cause qualitative mistakes.

1. Introduction

Nanobeams have immense potential applications in nanoelectromechanical systems (NEMS), for example, nanotube sensors [1] and resonators [2]. However, it is still an open question to model precisely nanobeams' mechanical properties [3–4]. There are two crucial characteristics in the mechanical properties of nanostructures. One of them is the small-scale effect that reveals that the mechanical properties and the geometric size are strongly related when a structure's size is down to the nanometer scale [5–11]. Another is the nonlinear elastic property determining the beam's overall mechanical behaviors [12–16]. The nonlinearity includes geometrical and material nonlinearity. There are many studies on the small-scale effect of nanobeams [17–21]. However, researchers have rarely paid attention to the material nonlinearity of nanobeams [22]. Nanobeam's nonlinearity in the thermal–electro-mechanical coupling also is a required field [23–24]. Researchers have usually modified the classical continuum mechanics to capture the small-scale effect through three different paths: the nonlocal stress gradient model $\left[1-\left(e_0a\right)^2\nabla^2\right]\sigma_{ij}=\bar{\sigma}_{ij}$ [7], the strain gradient model $\bar{\sigma}_{ij}=\left[1-\left(e_0a\right)^2\nabla^2\right]\bar{\varepsilon}_{ij}$ [9, 25–26], and the surface stress model [27]. Here $\bar{\sigma}_{ij}$ and $\bar{\varepsilon}_{ij}$ are the local stress and strain; σ_{ij} is the non-local stress; e_0 is a small-scale parameter; and is the material characteristic length which is the Carbon-Carbon bonding length for SWCNTs. The stress or strain gradient models have been widely used to study carbon nanotubes (CNTs) and graphene [28–30]. Since the mechanical properties of graphene and CNTs have lacked thorough understanding based on quantum mechanics [32], determining the scale parameter e_0 is still a controversial open question [5, 31]. Researchers calculated nonlinear elastic parameters for some materials through molecular dynamics (MD) and density functional theory (DFT), for example, CNTs [16], graphene [14], and silicon nanowires [13]. Because the material nonlinearity may cause complicated mechanical models, it has been neglected in exciting studies. Nonetheless, few existing studies of graphene and SWCNTs have shown that the stain's cubic terms in the potential energy (corresponding to the quadratic terms in the stress-strain relationship) significantly affect their mechanical properties [22, 33]. The accurate understanding of nanostructure's mechanical properties is the basis of applications. Therefore, it is necessary to consider both the small-scale effect and the material nonlinearity comprehensively. Under the Euler-Bernoulli assumption of displacements, the

present paper will propose two theories including the nonlocal effect and the material nonlinearity, to accurately characterize the nanobeam's mechanical properties for different boundary conditions.

2. Mathematical Modes

We restrict our attention to slender beams in the present research. Hence the Euler-Bernoulli hypothesis is employed [34]: the cross-sections perpendicular to the centroid locus before deformation remain plane and perpendicular to the deformed locus and suffer no strain in their planes. Under this hypothesis, only the beam's longitudinal (-direction) strain component, ε_{xx}, is considered, as shown in Fig. 1. Existing atomic calculations show that the potential energies of graphene and silicon materials contain at least the strain's cubic nonlinear terms [12–13]. Geometrical, y,an SWCNT can be viewed as a graphene sheet that has been rolled into a tube. Thus the stress-strain relationship of big diameter SWCNTs may be consistent with graphene. This was confirmed by MD simulations [16]. For simplicity, we assume that the beam's strain is finite but small, so only cubic nonlinear terms of the potential energy are kept, and the local longitudinal stress can be expressed as $\sigma_{xx} = \sigma_{xx}^{0} + E\varepsilon_{xx} + D\varepsilon_{xx}^{2}$ [12, 15–16, 22]. Here, σ_{xx}^{0} is the initial prestress, and are the second-order and third-order elastic coefficients, respectively. Following the nonlocal differential constitutive relationship, the nanobeam's nonlocal constitutive relationship with the material nonlinearity can write as

$$\left[1 - \mu^2 \nabla^2\right]\sigma_{xx} = \sigma_{xx} = \sigma_{xx}^{0} + E\varepsilon_{xx} + D\varepsilon_{xx}^{2}$$

1

,

here $\mu = e_0 a$. For establishing theories of nanobeams, it is necessary to give the beam's strain-displacement relation according to different boundary constraints [34–36]. We consider two conditions in this paper. First, if the two ends of beams are immovable along the direction, such as clamped-clamped or hinged-hinged beams, the effect of axial elongation needs to be considered at this point. Second, beams are inextensional, such as simply supported or clamped-free beams. The present paper will establish motion equations for two conditions, respectively.

2.1. Model with axial extensional effect

If the two ends of a beam cannot move along the -axis, such as hinged-hinged or clamped-clamped beams, the bending deformations may induce the axial extension. So the axial strain is [34]

$$\varepsilon_{xx} = \frac{\partial u}{\partial x} + \frac{1}{2}\left(\frac{\partial w}{\partial x}\right)^2 - y\frac{\partial^2 w}{\partial x^2}$$

2

.

Here, and are axial displacements of the beam in the and directions respectively, as shown in Fig. 1. Substituting Eq. (2) into the expression of local stress, $\bar{\sigma}_{xx} = \bar{\sigma}^{0}_{xx} + E\bar{\varepsilon}_{xx} + D\bar{\varepsilon}^{2}_{xx}$, has the local axial force and bending moment as

$$\bar{N} = \int_A \bar{\sigma}_{xx} dA = -N_0 + EA\left[\frac{\partial u}{\partial x} + \frac{1}{2}\left(\frac{\partial w}{\partial x}\right)^2\right] + ID\left(\frac{\partial^2 w}{\partial x^2}\right)^2 + DA\left[\frac{\partial u}{\partial x} + \frac{1}{2}\left(\frac{\partial w}{\partial x}\right)^2\right]^2,$$

3

$$\bar{M} = \int_A yE\bar{\sigma}_{xx} dA = -EI\frac{\partial^2 w}{\partial x^2} - 2ID\left[\frac{\partial u}{\partial x} + \frac{1}{2}\left(\frac{\partial w}{\partial x}\right)^2\right]\frac{\partial^2 w}{\partial x^2}.$$

4

Here, $A = \pi dh$ and $I = \pi d^3 h/8$ are the beam's cross-sectional area and the inertia moment of SWCNTs. is the SWCNT's diameter, and is the thickness; $N_0 = \int_A \bar{\sigma}^{0}_{xx} dA$ is the initial axial load at the ends, as shown in Fig. 1. The quartic terms of can neglect for slender beams [34], and notices $\partial u/\partial x = \mathrm{O}(\partial w/\partial x)^2$ [35], the force reduces to

$$\bar{N} = \int_A \bar{\sigma}_{xx} dA = -N_0 + EA\left[\frac{\partial u}{\partial x} + \frac{1}{2}\left(\frac{\partial w}{\partial x}\right)^2\right] + ID\left(\frac{\partial^2 w}{\partial x^2}\right)^2.$$

5

The equations of motion with the extensional effect are [34]

$$\frac{\partial N}{\partial x} = m\frac{\partial^2 u}{\partial t^2},$$

6

$$\frac{\partial^2 M}{\partial x^2} + N\frac{\partial^2 w}{\partial x^2} = m\frac{\partial^2 w}{\partial t^2} + \bar{F}(x, t).$$

7

Here is the beam's mass per unit length, and are the nonlocal axial force and the nonlocal moment. Taking into account Eq. (4) and Eq. (5), the non-local constitutive Eq. (1) transforms into

$$M - \mu^2 \frac{\partial^2 M}{\partial x^2} = -EI\frac{\partial^2 w}{\partial x^2} - 2ID\left[\frac{\partial u}{\partial x} + \frac{1}{2}\left(\frac{\partial w}{\partial x}\right)^2\right]\frac{\partial^2 w}{\partial x^2},$$

8

$$N - \mu^2 \frac{\partial^2 N}{\partial x^2} = -N_0 + ID\left(\frac{\partial^2 w}{\partial x^2}\right)^2 + EA\left[\frac{\partial u}{\partial x} + \frac{1}{2}\left(\frac{\partial w}{\partial x}\right)^2\right].$$

9

Substituting Eq. (6) and Eq. (7) into Eq. (8) and Eq. (9), gets

$$M - \mu^2\left(m\frac{\partial^2 w}{\partial t^2} - N\frac{\partial^2 w}{\partial x^2} + \mathbb{F}\right) = -EI\frac{\partial^2 w}{\partial x^2} - 2ID\left[\frac{\partial u}{\partial x} + \frac{1}{2}\left(\frac{\partial w}{\partial x}\right)^2\right]\frac{\partial^2 w}{\partial x^2},$$

10

$$N - \mu^2\frac{\partial}{\partial x}\left(m\frac{\partial^2 u}{\partial t^2}\right) = -N_0 + ID\left(\frac{\partial^2 w}{\partial x^2}\right)^2 + EA\left[\frac{\partial u}{\partial x} + \frac{1}{2}\left(\frac{\partial w}{\partial x}\right)^2\right].$$

11

Differentiates Eq. (10) twice with respect to , then substitutes it into the Eq. (7), gets

$$-EI\frac{\partial^4 w}{\partial x^4} + N\frac{\partial^2 w}{\partial x^2} - 2ID\frac{\partial^2}{\partial x^2}\left\{\left[\frac{\partial u}{\partial x} + \frac{1}{2}\left(\frac{\partial w}{\partial x}\right)^2\right]\frac{\partial^2 w}{\partial x^2}\right\}$$

$$+\mu^2\frac{\partial^2}{\partial x^2}\left(m\frac{\partial^2 w}{\partial t^2} - N\frac{\partial^2 w}{\partial x^2} + \mathbb{F}\right) = m\frac{\partial^2 w}{\partial t^2} + \mathbb{F}(x, t).$$

12

From Eq. (11), has

$$N = \mu^2\frac{\partial}{\partial x}\left(m\frac{\partial^2 u}{\partial t^2}\right) - N_0 + ID\left(\frac{\partial^2 w}{\partial x^2}\right)^2 + EA\left[\frac{\partial u}{\partial x} + \frac{1}{2}\left(\frac{\partial w}{\partial x}\right)^2\right].$$

13

Substituting Eq. (13) into Eq. (12), and ignoring the inertia term $\partial^2 u/\partial t^2$, gets the lateral motion equation as follows.

$$-EI\frac{\partial^4 w}{\partial x^4}+\left\{-N_0+ID\left(\frac{\partial^2 w}{\partial x^2}\right)^2+EA\left[\frac{\partial u}{\partial x}+\frac{1}{2}\left(\frac{\partial w}{\partial x}\right)^2\right]\right\}\frac{\partial^2 w}{\partial x^2}$$

$$-2ID\frac{\partial^2}{\partial x^2}\left\{\left[\frac{\partial u}{\partial x}+\frac{1}{2}\left(\frac{\partial w}{\partial x}\right)^2\right]\frac{\partial^2 w}{\partial x^2}\right\}-\mu^2\frac{\partial^2}{\partial x^2}\left\{\left[-N_0+ID\left(\frac{\partial^2 w}{\partial x^2}\right)^2\right.\right.$$

$$\left.\left.+EA\left[\frac{\partial u}{\partial x}+\frac{1}{2}\left(\frac{\partial w}{\partial x}\right)^2\right]\right]\frac{\partial^2 w}{\partial x^2}\right\}=m\left(\frac{\partial^2 w}{\partial t^2}-\mu^2\frac{\partial^4 w}{\partial t^2\partial x^2}\right)+\ddot{F}-\mu^2\frac{\partial^2 \ddot{F}}{\partial x^2}.$$

14

Differentiates Eq. (13) with respect to , then substitutes it into Eq. (6), gets

$$ID\frac{\partial}{\partial x}\left(\frac{\partial^2 w}{\partial x^2}\right)^2+EA\frac{\partial}{\partial x}\left[\frac{\partial u}{\partial x}+\frac{1}{2}\left(\frac{\partial w}{\partial x}\right)^2\right]=m\frac{\partial^2 u}{\partial t^2}-\mu^2 m\frac{\partial^4 u}{\partial t^2\partial x^2}.$$

15

Eq. (14) and Eq. (15) are the nanobeam's plane motion equations with the nonlocal nonlinear constitutive and the extensional effect. Their boundary conditions of displacements are the same as the classical beam theory. If we considered only bending motion, the inertia terms of Eq. (15) can be ignored [35–36], then Eq. (15) simplifies as

$$\frac{\partial^2 u}{\partial x^2}=-\frac{\partial}{\partial x}\left[\frac{1}{2}\left(\frac{\partial w}{\partial x}\right)^2+\lambda\left(\frac{\partial^2 w}{\partial x^2}\right)^2\right]$$

16

,

here $\lambda = DI/EA$. Integrating Eq. (16) with respect to , gets

$$\frac{\partial u}{\partial x} = -\frac{1}{2}\left(\frac{\partial w}{\partial x}\right)^2 - \lambda\left(\frac{\partial^2 w}{\partial x^2}\right)^2 + C_1(t),$$

$$u = -\frac{1}{2}\int_0^x \left[\left(\frac{\partial w}{\partial s}\right)^2 + 2\lambda\left(\frac{\partial^2 w}{\partial s^2}\right)^2\right] ds + C_1(t)x + C_2(t).$$

17

Where C_1 and C_2 are functions of time , which can be determined by imposing boundary conditions on . For a beam with two unmovable ends, gets [35–36]

$$C_1(t) = \frac{1}{2l}\int_0^l \left[\left(\frac{\partial w}{\partial x}\right)^2 + 2\lambda\left(\frac{\partial^2 w}{\partial x^2}\right)^2\right] dx, \quad C_2 = 0.$$

18

Substituting Eq. (17) into Eq. (14) and omitting the quartic terms of , gets

$$m\left(\frac{\partial^2 w}{\partial t^2} - \mu^2\frac{\partial^4 w}{\partial t^2 \partial x^2}\right) + C\frac{\partial w}{\partial t} + EI\frac{\partial^4 w}{\partial x^4} + N_0\left(\frac{\partial^2 w}{\partial x^2}\right.$$

$$\left. - \mu^2\frac{\partial^4 w}{\partial x^4}\right) - 2\lambda ID\frac{\partial^2}{\partial x^2}\left(\frac{\partial^2 w}{\partial x^2}\right)^3 - \frac{EA}{2l}\left[\frac{\partial^2 w}{\partial x^2} - \left(2\lambda + \mu^2\right)\frac{\partial^4 w}{\partial x^4}\right]$$

$$\int_0^l \left[\left(\frac{\partial w}{\partial x}\right)^2 + 2\lambda\left(\frac{\partial^2 w}{\partial x^2}\right)^2\right] dx = F + \mu^2\frac{\partial^2 F}{\partial x^2}.$$

19

In Eq. (19), we add a linear damping term $C\partial w/\partial t$. For a hinged-hinged beam, the boundary conditions are [34–36]

w\left({0,t} \right)=w\left({l,t} \right)=\frac{{{\partial ^2}w}}{{\partial {x^2}}}\left({0,t} \right)=\frac{{{\partial ^2}w}}{{\partial {x^2}}}\left({l,t} \right)=0.

20

2.2. The model with the inextensional effect

If a nanobeam has a fixed or hinged end and another is free or sliding, the beam is inextensional. At this point, the strain can write as [34–36]

„ (21)

Substituting Eq. (21) into the local nonlinear constitutive equation, {\bar {\sigma }_{xx}}=\bar {\sigma }_{{xx}}^{0}+E{\bar {\varepsilon }_{xx}}+D\bar {\varepsilon }_{{xx}}^{2}, and noting \int\limits_{A} {{y^3}dA} =0 for symmetrical cross-sections, the local axial force and the moment are

\bar {N}=\int\limits_{A} {{{\bar {\sigma }}_{xx}}dA} = - {N_0} - ID{\left({\frac{{{\partial ^2}w}}{{\partial {x^2}}}} \right)^2}
22
,
\bar {M}=\int\limits_{A} {yE{\varepsilon _{xx}}dA} = - EI\left[{\frac{{{\partial ^2}w}}{{\partial {x^2}}}+\frac{1}{2}{{\left({\frac{{\partial w}}{{\partial x}}} \right)}^2}\left({\frac{{{\partial ^2}w}}{{\partial {x^2}}}} \right)} \right].
23

Analogous to the virtual work principle of the classical beam theory [34], has

\frac{{\partial N}}{{\partial x}}=m\frac{{{\kern 1pt} {\partial ^2}u}}{{\partial {t^2}}}
24
,
\begin{gathered} \frac{{{\partial ^2}M}}{{\partial {x^2}}}+\frac{1}{2}\frac{\partial }{{\partial x}}\left[{\frac{{\partial M}}{{\partial x}}{{\left({\frac{{\partial w}}{{\partial x}}} \right)}^2}} \right]+N\frac{{{\partial ^2}w}}{{\partial {x^2}}}=m\frac{{{\partial ^2}w}}{{\partial {t^2}}} \hfill \\ +\frac{m}{2}\frac{\partial }{{\partial x}}\left\{ {\frac{{\partial w}}{{\partial x}}\int\limits_{l}^{s} {\left[{\frac{{{\partial ^2}}}{{\partial {t^2}}}\int\limits_{l}^{s} {{{\left({\frac{{\partial w}}{{\partial x}}} \right)}^2}ds} } \right]ds} } \right\}+\bar {F}\left({x,t} \right). \hfill \\ \end{gathered}
25

For simplicity, we ignore the ’s nonlinear term in Eq. (25), and gets

\frac{{{\partial ^2}M}}{{\partial {x^2}}} \approx m\frac{{{\partial ^2}w}}{{\partial {t^2}}}+\frac{1}{2}m\frac{\partial }{{\partial x}}\left\{ {\frac{{\partial w}}{{\partial x}}\int\limits_{l}^{s} {\left[{\frac{{{\partial ^2}}}{{\partial {t^2}}}\int\limits_{l}^{s} {{{\left({\frac{{\partial w}}{{\partial x}}} \right)}^2}ds} } \right]ds} } \right\} - N\frac{{{\partial ^2}w}}{{\partial {x^2}}}+\bar {F}\left({x,t} \right).
26

Neglecting m{\partial ^2}u/\partial {t^2}, Eq. (24) can be simplified to \partial N/\partial x=0, hence gets

{\partial ^2}N/\partial {x^2}=0
27

Substituting Eq. (21) into Eq. (1), the nonlocal constitutive relationship is transformed into

$$M - {\mu ^2}\frac{{{\partial ^2}M}}{{\partial {x^2}}}= - EI\left[{\frac{{{\partial ^2}w}}{{\partial {x^2}}}+\frac{1}{2}{{\left({\frac{{\partial w}}{{\partial x}}} \right)}^2}\left({\frac{{{\partial ^2}w}}{{\partial {x^2}}}} \right)} \right]$$

28

,

$$N - {\mu ^2}\frac{{{\partial ^2}N}}{{\partial {x^2}}}= - {N_0}+ID{\left({\frac{{{\partial ^2}w}}{{\partial {x^2}}}} \right)^2}$$

29

.

Substituting Eq. (26) and Eq. (27) into Eq. (28) and Eq. (29), gets

$$\begin{gathered} M= - EI\left[{\frac{{{\partial ^2}w}}{{\partial {x^2}}}+\frac{1}{2}{{\left({\frac{{\partial w}}{{\partial x}}} \right)}^2}\left({\frac{{{\partial ^2}w}}{{\partial {x^2}}}} \right)} \right] - {\mu ^2}N\frac{{{\partial ^2}w}}{{\partial {x^2}}}+{\mu ^2}\bar {F}\left({x,t} \right) \hfill \\ +{\mu ^2}\left\{ {m\frac{{{\partial ^2}w}}{{\partial {t^2}}}+\frac{m}{2}\frac{\partial }{{\partial x}}\left\{ {\frac{{\partial w}}{{\partial x}}\int\limits_{l}^{s} {\left[{\frac{{{\partial ^2}}}{{\partial {t^2}}}\int\limits_{l}^{s} {{{\left({\frac{{\partial w}}{{\partial x}}} \right)}^2}ds} } \right]ds} } \right\}} \right\}, \hfill \\ \end{gathered}$$

30

$$N= - {N_0}+ID{\left({\frac{{{\partial ^2}w}}{{\partial {x^2}}}} \right)^2}$$

31

.

Differentiates Eq. (30) once and twice with respect to , then substitutes the outcomes and Eq. (31) into Eq. (25), gets

$$\begin{gathered} - EI\frac{{{\partial ^4}w}}{{\partial {x^4}}} - {N_0}\left({\frac{{{\partial ^2}w}}{{\partial {x^2}}} - {\mu ^2}\frac{{{\partial ^4}w}}{{\partial {x^4}}}} \right)+\frac{{{\mu ^2}{N_0}}}{2}\frac{\partial }{{\partial x}}\left[{{{\left({\frac{{\partial w}}{{\partial x}}} \right)}^2}\frac{{{\partial ^3}w}}{{\partial {x^3}}}} \right] \hfill \\ \left. { - EI\frac{\partial }{{\partial x}}\left[{\frac{{\partial w}}{{\partial x}}{{\left({\frac{{{\partial ^2}w}}{{\partial {x^2}}}} \right)}^2}} \right.+{{\left({\frac{{\partial w}}{{\partial x}}} \right)}^2}\frac{{{\partial ^3}w}}{{\partial {x^3}}}} \right]+ID\left[{{{\left({\frac{{{\partial ^2}w}}{{\partial {x^2}}}} \right)}^3} - {\mu ^2}\frac{{{\partial ^2}}}{{\partial {x^2}}}{{\left({\frac{{{\partial ^2}w}}{{\partial {x^2}}}} \right)}^3}} \right] \hfill \\ =m\frac{{{\partial ^2}w}}{{\partial {t^2}}} - {\mu ^2}m\frac{{{\partial ^4}w}}{{\partial {t^2}\partial {x^4}}} - \frac{{{\mu ^2}m}}{2}\frac{\partial }{{\partial x}}\left[{\frac{{{\partial ^3}w}}{{\partial {t^2}\partial x}}{{\left({\frac{{\partial w}}{{\partial x}}} \right)}^2}} \right]+\left({\frac{m}{2}\frac{\partial }{{\partial x}} - \frac{{{\mu ^2}m}}{2}\frac{{{\partial ^3}}}{{\partial {x^3}}}} \right) \hfill \\ \left\{ {\frac{{\partial w}}{{\partial x}}\int\limits_{l}^{s} {\left[{\frac{{{\partial ^2}}}{{\partial {t^2}}}\int\limits_{l}^{s} {{{\left({\frac{{\partial w}}{{\partial x}}} \right)}^2}ds} } \right]ds} } \right\}+\bar {F} - {\mu ^2}\left\{ {\frac{{{\partial ^2}\bar {F}}}{{\partial {x^2}}}+\frac{1}{2}\frac{\partial }{{\partial x}}\left[\right.$$

{\frac{{\partial \bar {F}}}{{\partial x}}{{\left({\frac{{\partial w}}{{\partial x}}} \right)}^2}} \right]} \right\}. \hfill \\ \end{gathered}
32

In Eq. (32), the nonlinear terms of only keep up to cubic terms. Because the nonlinear inertia terms can omit for slender beams [36], Eq. (32) can simplify as

\begin{gathered} m\left({\frac{{{\partial ^2}w}}{{\partial {t^2}}} - {\mu ^2}\frac{{{\partial ^4}w}}{{\partial {t^2}\partial {x^4}}}} \right)+C\frac{{\partial w}}{{\partial t}}+EI\frac{{{\partial ^4}w}}{{\partial {x^4}}}+ {N_0}\left({\frac{{{\partial ^2}w}}{{\partial {x^2}}} - {\mu ^2}\frac{{{\partial ^4}w}}{{\partial {x^4}}}} \right) \hfill \\ - \frac{{{\mu ^2}{N_0}}}{2}\frac{\partial }{{\partial x}}\left[{{{\left({\frac{{\partial w}}{{\partial x}}} \right)}^2}\frac{{{\partial ^3}w}}{{\partial {x^3}}}} \right]+EI\frac{\partial }{{\partial x}}\left[{\frac{{\partial w}}{{\partial x}}{{\left({\frac{{{\partial ^2}w}}{{\partial {x^2}}}} \right)}^2}+{{\left({\frac{{\partial w}} {{\partial x}}} \right)}^2}\frac{{{\partial ^3}w}}{{\partial {x^3}}}} \right] \hfill \\ - ID\left[{{{\left({\frac{{{\partial ^2}w}}{{\partial {x^2}}}} \right)}^3} - {\mu ^2}\frac{{{\partial ^2}}}{{\partial {x^2}}}{{\left({\frac{{{\partial ^2}w}}{{\partial {x^2}}}} \right)}^3}} \right]=\bar {F} - {\mu ^2}\left\{ {\frac{{{\partial ^2}\bar {F}}}{{\partial {x^2}}}+\frac{1}{2}\frac{\partial }{{\partial x}}\left[{\frac{{\partial \bar {F}}}{{\partial x}}{{\left({\frac{{\partial w}}{{\partial x}}} \right)}^2}} \right]} \right\} \hfill \\ \end{gathered}
33

The displacement boundary conditions of Eq. (33) are the same as those of classical beams. For example, the conditions of simply supported beams are

w\left({0,t} \right)=w\left({l,t} \right)=\frac{{{\partial ^2}w}}{{\partial {x^2}}}\left({0,t} \right)=\frac{{{\partial ^2}w}}{{\partial {x^2}}}\left({l,t} \right)=0.
34

Below we will analyze Eq. (19) and Eq. (33). The above two models can divide into four categories: the classical nonlinear model (CNM) for D=0and \mu =0, the nonlinear constitutive model (NCM) for D \ne 0and \mu =0, the nonlocal nonlinear model (NNM) for D=0and \mu \ne 0, and the nonlocal nonlinear constitutive model (NNCM) for D \ne 0and \mu \ne 0.

3. Solutions Of Models

Introducing dimensionless variables in Eq. (19) and Eq. (33) is convenient. Lets \bar {x}=x/l, \bar {w}=w/l, \bar {x}=x/l, \bar {t}=t/{\omega _0}, and \omega _{0}^{2}={\pi ^4}EI{\left({{l^4}m} \right)^{ - 1}}. Assumes the loads are uniform, namely \bar {F}\left(x \right)=\text{c}\text{o}\text{n}\text{s}\text{t}, so {\partial ^2}\bar {F}/\partial {x^2}=0. Eq. (19) for the extensibility effect can rewrite as

\begin{gathered} \frac{{{\partial ^2}}}{{\partial {{\bar {t}}^2}}}\left({\bar {w} - \frac{{{\mu ^2}}}{{{l^2}}}\frac{{{\partial ^2}\bar {w}}}{{\partial {{\bar {x}}^2}}}} \right)+\frac{C}{{m{\omega _0}}}\frac{{\partial \bar {w}}}{{\partial t}}+\frac{1}{{{\pi ^4}}}\frac{{{\partial ^4}\bar {w}}}{{\partial {{\bar {x}}^4}}} \hfill \\

$$+\frac{{{N_0}}}{{m\omega _{0}^{2}{l^2}}}\left({\frac{{{\partial ^2}\bar {w}}}{{\partial {{\bar {x}}^2}}}\left. { - \frac{{{\mu ^2}}}{{{l^2}}}\frac{{{\partial ^4}\bar {w}}}{{\partial {{\bar {x}}^4}}}} \right) - \frac{{2\lambda ID}}{{m\omega _{0}^{2}{l^6}}}\frac{{{\partial ^2}}}{{\partial {{\bar {x}}^2}}}{{\left({\frac{{{\partial ^2}\bar {w}}}{{\partial {{\bar {x}}^2}}} \right)}^3}} \right. \hfill \\ - \frac{{EA}}{{2m\omega _{0}^{2}{l^2}}}\left({\frac{{{\partial ^2}\bar {w}}}{{\partial {{\bar {x}}^2}}} \right.\left. { - \frac{{2\lambda +{\mu ^2}}}{{{l^2}}}\frac{{{\partial ^4}\bar {w}}}{{\partial {{\bar {x}}^4}}} \right)\int\limits_{0}^{1} {\left[{{{\left({\frac{{\partial \bar {w}}}{{\partial \bar {x}}}} \right)}^2}+\frac{{2\lambda }}{{{l^2}}}{{\left({\frac{{{\partial ^2}\bar {w}}}{{\partial {{\bar {x}}^2}}} \right)}^2}} \right]d{\kern 1pt} \bar {s}} =\frac{{\bar {F}}}{{m\omega _{0}^{2}l}}. \hfill \\ \end{gathered}$$

35

Eq. (33) for inextensible beams can rewrite as

$$\begin{gathered} \frac{{{\partial ^2}\bar {w}}}{{\partial {{\bar {t}}^2}}} - \frac{{{\mu ^2}}}{{{l^2}}}\frac{{{\partial ^4}\bar {w}}}{{\partial {{\bar {t}}^2}\partial {{\bar {x}}^2}}}+\frac{C}{{m{\omega _0}}}\frac{{\partial \bar {w}}}{{\partial t}}+\frac{1}{{{\pi ^4}}}\frac{{{\partial ^4}\bar {w}}}{{\partial {{\bar {x}}^4}}}+\frac{{{N_0}}}{{m\omega _{0}^{2}{l^2}}}\left({\frac{{{\partial ^2}\bar {w}}}{{\partial {{\bar {x}}^2}}} - \frac{{{\mu ^2}}}{{{l^2}}}\frac{{{\partial ^4}\bar {w}}}{{\partial {{\bar {x}}^4}}} \right) \hfill \\ - \frac{{{\mu ^2}{N_0}}}{{2m\omega _{0}^{2}{l^4}}}\frac{\partial }{{\partial \bar {x}}}\left[{{{\left({\frac{{\partial \bar {w}}}{{\partial \bar {x}}}} \right)}^2}\frac{{{\partial ^3}\bar {w}}}{{\partial {{\bar {x}}^3}}} \right]+\frac{{EI}}{{2m\omega _{0}^{2}{l^4}}}\frac{\partial }{{\partial \bar {x}}}\left[{\frac{{\partial \bar {w}}}{{\partial \bar {x}}}{{\left({\frac{{{\partial ^2}\bar {w}}}{{\partial {{\bar {x}}^2}}}} \right)}^2}} \right. \hfill \\ \left. {+{{\left({\frac{{\partial \bar {w}}}{{\partial \bar {x}}}} \right)}^2}\frac{{{\partial ^3}\bar {w}}}{{\partial {{\bar {x}}^3}}}} \right] - \frac{{DI}}{{m\omega _{0}^{2}{l^4}}}\left[{{{\left({\frac{{{\partial ^2}\bar {w}}}{{\partial {{\bar {x}}^2}}}} \right)}^3} - \frac{{{\mu ^2}}}{{{l^2}}}\frac{{{\partial ^2}}}{{\partial {{\bar {x}}^2}}}{{\left({\frac{{{\partial ^2}\bar {w}}}{{\partial {{\bar {x}}^2}}}} \right)}^3}} \right]=\frac{{\bar {F}}}{{m\omega _{0}^{2}l}}. \hfill \\ \end{gathered}$$

36

For simplicity, we use hinged-hinged and simply supported beams as examples to discuss the extensible and inextensible beams correspondingly. Hence their normalized boundary conditions are identical:

$$\bar {w}\left({0,\bar {t}} \right)=\bar {w}\left({1,\bar {t}} \right)=\frac{{{\partial ^2}\bar {w}}}{{\partial {{\bar {x}}^2}}}\left({0,\bar {t}} \right)=\frac{{{\partial ^2}\bar {w}}}{{\partial {{\bar {x}}^2}}}\left({1,\bar {t}} \right)=0$$

37

.

It is challenging to solve nonlinear Eq. (35) or Eq. (36) accurately. There are two common approaches to solving a nonlinear partial differential equation approximately. One of them is that the partial differential equation is reduced to nonlinear ordinary differential equations through Galerkin method, and then the equations are solved using perturbation methods [34–37]. The second is to solve the nonlinear partial

differential equation using perturbation methods directly. The direct multiscale method is an essential improvement of the classical perturbation methods, and it has been widely used to directly solve nonlinear partial differential equations more accurately than the first methods [37]. Nayfeh [38–40], Luongo [41, 42], and Lacarbonara [43–46] and their collaborators' works may be substantial for the direct multiscale method. We apply the Galerkin and the multi-scale methods to solve the equations for simplicity. In fact, the two methods have widely applied to nonlinear equations of structures [18, 20–22, 47–50]. Under boundary conditions Eqs. (37), the approximate solutions of Eq. (35) and Eq. (36) can be written as

$$\bar {w}=\sum\limits_{{n=1}}^{\infty } {{\bar {\eta }}_n}\left({\bar {t}} \right)\sin n\pi \bar {x}} \tag{38}$$

.

A set of ordinary differential equations can obtain through the Galerkin truncation [34, 36]: substitutes Eq. (38) into Eq. (35) or Eq. (36) respectively, then $\sin \left({n\pi \bar {x}} \right)$ is multiplied by both sides of the equations, and integrates in the interval $\left[{0,1} \right]$. For simplicity, we only takes the first term of Eq. (38) and let ${\bar {\eta }}_1}=\eta$, get

$${m_j}\ddot {\eta }+{c_j}\dot {\eta }+{k_j}\eta +{d_j}{\eta ^3}=f,\quad j=1,2. \tag{39}$$

Here j=1 indicates the hinged-hinged beams, and j=2 indicates the simply supported beams. The parameters in Eqs. (39) are

$$\begin{gathered} {m_1}={m_2}=1+\frac{{{\pi ^2}{\mu ^2}}}{{{l^2}}},\quad {c_1}={c_2}=\frac{C}{{m{\omega _0}}},\quad {k_1}={k_2}=1 - \frac{{{N_0}{\pi ^2}}}{{m\omega _{0}^{2}{l^2}}}\left({1+\frac{{{\pi ^2}{\mu ^2}}}{{{l^2}}}} \right), \hfill \\ {d_1}=\frac{{{\pi ^4}EA}}{{4m\omega _{0}^{2}{l^2}}}{\left({1+\frac{{2{\pi ^2}\lambda }}{{{l^2}}}} \right)^2} - \frac{{3{\pi ^8}\lambda ID}}{{2m\omega _{0}^{2}{l^6}}}+\frac{{{\pi ^4}EA{\mu ^2}}}{{4m\omega _{0}^{2}{l^4}}}\left({1+\frac{{2{\pi ^2}\lambda }}{{{l^2}}}} \right), \hfill \\ {d_2}= - \frac{{3{\pi ^6}{\mu ^2}{N_0}}}{{8m\omega _{0}^{2}{l^4}}}+\frac{{{\pi ^6}EI}}{{6m\omega _{0}^{2}{l^4}}}+\frac{{3{\pi ^6}DI}}{{4m\omega _{0}^{2}{l^4}}}\left({1+\frac{{{\pi ^2}{\mu ^2}}}{{{l^2}}}} \right),\;F=\frac{{4\bar {F}}}{{\pi m\omega _{0}^{2}l}}. \hfill \\ \end{gathered} \tag{40}$$

Eqs. (40) indicate that the linear coefficients of the two models are the same, but the nonlinear coefficients are different. Moreover, the non-local effect and the material nonlinearity are coupled in nonlinear terms. ${d_1}$ demonstrates that the influence of the material nonlinearity will decrease accompanying the increase of beam's length, as hinged-hinged SWCNTs shown in Fig. 2. If we neglect the nonlocal effect, the material nonlinearity's influence on ${d_2}$ is invariant accompanying the length's change due to $\omega _{0}^{2}{l^4}={\pi ^4}EI/m$, as simply supported SWCNTs shown in Fig. 9.

The nonlinear terms, which are induced by the finite deformations and the non-local effect, produce a hardening effect in two models due to {\mu ^2}>0. On the other hand, the nonlinear terms induced by the material nonlinearity have a softening effect in two models due to D<0 for SWCNTs. It is interesting for hinged-hinged SWCNTs that the hardening effect will be smaller than the softening effect for the small-length tubes, as shown in Fig. 2. The following discussions will show that this competitive relationship between the softening and the hardening impacts the mechanical behavior of SWCNTs significantly.

Neglecting the inertia and damping terms in Eqs. (39), static bending deformations of the beams' middle points are obtained as

{k_j}\eta +{d_j}{\eta ^3}=F,\quad j=1,2.
41

In the following, we will research the mechanical behaviors of hinged-hinged beams and simply supported beams according to Eq. (39) and Eq. (41), respectively.

We rewrite Eqs. (39) as

\ddot {\eta }+{\bar {c}_j}\dot {\eta }+\bar {\omega }_{j}^{2}\eta +{\bar {d}_j}{\eta ^3}=\bar {f},\quad j=1,2
42
,

here {\bar {c}_j}={c_j}/{m_j}, {\omega ^2}={k_1}/{m_j}, {\bar {d}_j}={d_j}/{m_j}, \bar {f}={\bar {f}_j}=F/{m_j}. The multiple scale method [36], which is widely used to solve weak nonlinear differential equations for macro-structures, will be applied to solve Eq. (42). Lets {\bar {c}_j}={\varepsilon ^2}{c_j}, \bar {f}= {\varepsilon ^3}f\cos \left({\Omega \bar {t}} \right), gives

\ddot {\eta }+\omega _{j}^{2}\eta +{\varepsilon ^2}{c_j}\dot {\eta }+{\bar {d}_j}{\eta ^3}={\varepsilon ^3}f\cos \left({\Omega \bar {t}} \right),\quad j=1,2.
43
.

Supposes

\eta \left({t;\varepsilon } \right)=\varepsilon {\eta _1}\left({{T_0},{T_2}} \right)+{\varepsilon ^3}{\eta _3}\left({{T_0},{T_2}} \right)
44
,

and substitutes it into Eq. (43), then equates the coefficients of \varepsilon and {\varepsilon ^3} on both sides, has

\varepsilon :\quad D_{0}^{2}{\eta _1}+\omega _{i}^{2}{\eta _1}=0,
45

\begin{gathered} {\varepsilon ^3}:\quad D_{0}^{2}{\eta _3}+\omega _{j}^{2}{\eta _3}= - 2{D_0}{D_2}{\eta _1} \hfill \\ \quad - 2{c_j}{D_0}{\eta _1} - {{\bar {d}}_j}\eta _{1}^{3}+\frac{1}{2}f\exp \left({i\Omega {T_0}} \right), \hfill \\ \end{gathered}
46

where {D_0}=d/d{T_0}, {D_1}=d/d{T_1} and D_{0}^{2}={d^2}/dT_{0}^{2}. The solution of Eq. (45) is

{\eta _1}=A\left({{T_2}} \right)\exp \left({i{\omega _j}{T_0}} \right)+CC
47
,

here, *CC* means the complex conjugate. Substituting Eq. (47) into Eq. (46), gets

\begin{gathered} D_{0}^{2}{\eta _3}+\omega _{j}^{2}{\eta _3}=\frac{1}{2}f\exp \left({i{\kern 1pt} \Omega {T_0}} \right) \hfill \\ - \left[{i2\omega \left({A^{\prime}+{c_j}A} \right)} \right.\left. {+3{{\bar {d}}_j}{A^2}\bar {A}} \right]\exp \left({i{\omega _j}{T_0}} \right)+NST. \hfill \\ \end{gathered}
48

Here the prime denotes the derivative with respect to {T_2}, and NST denotes non-secular terms [36]. When the load's frequency \Omega approaches the nanobeam's modal frequency {\omega _j} (primary resonance), the beam will appear a relatively large amplitude response. Under this condition, lets \Omega ={\omega _j}+{\varepsilon ^2}\sigma, so the solvable condition of Eq. (48) are

- i2{\omega _j}\left({A^{\prime}+cA} \right) - 3{d_j}{A^2}\bar {A}+\frac{1}{2}f\exp \left({i\sigma {T_2}} \right)=0,\quad j=1,2.
49
.

Letting A=\left({\alpha /2} \right)\exp \left({i\beta } \right), and substituting it into Eq. (49), then separating the real part and the imaginary part, gets

\begin{gathered} \alpha ^{\prime}= - {c_j}\alpha +\frac{f}{{2\omega }}\sin \gamma , \hfill \\ \alpha \gamma ^{\prime}=\sigma \alpha - \frac{3}{{8{\omega _i}}}{{\bar {d}}_j}{\alpha ^3}+\frac{f}{{2{\omega _j}}}\cos \gamma , \hfill \\ \end{gathered}
50

here \gamma =\sigma {T_2} - \beta. Steady-state motions occur when \alpha ^{\prime}=\gamma ^{\prime}=0, which corresponds to the singular points of Eqs. (50). The steady-state solutions can obtain from the following algebraic equations [36]

\left[{{c^2}+{{\left({\sigma - \frac{{3{{\bar {d}}_j}}}{{8\omega _{j}^{2}}}{\alpha ^2}} \right)}^2}} \right]{\alpha ^2}=\frac{{{f^{{\kern 1pt} 2}}}}{{4\omega _{j}^{2}}},\quad j=1,2
51

.

The stability of the steady-state solutions is judged by investigating the nature of the singular points of Eqs. (50). Lets a={a_0}+{a_1} and \gamma ={\gamma _0}+{\gamma _1}, and substitutes them into Eqs. (50), expands for small {a_1} and {\gamma _1}, and keeps linear terms in {a_1} and {\gamma _1}, then gets

\begin{gathered} {{\alpha ^{\prime}}_1}= - {c_j}{\alpha _1}+\frac{{{\gamma _1}f\cos {\gamma _0}}}{{2{\omega _j}}}, \hfill \\ {{\gamma ^{\prime}}_1}= - \left({\frac{{f\cos {\gamma _0}}}{{2{\omega _j}\alpha _{0}^{2}}}+\frac{{3{{\bar {d}}_j}{\alpha _0}}}{4}} \right){\alpha _1} - \frac{{{\gamma _1}f\sin {\gamma _0}}}{{2{\omega _j}{\alpha _0}}}. \hfill \\ \end{gathered}
52

Here, it is used in Eqs. (52) that {a_0} and {\gamma _0} are the singular points of Eqs. (50). The stability of steady-state motions depends on the coefficient matrix's eigenvalues of Eqs. (52). If the real parts of eigenvalues are greater than zero, the solutions are unstable [36]. Hence the steady-state motions are unstable if

c_{j}^{2}+\left({\frac{{3{d_j}\alpha _{0}^{2}}}{{8{\omega _j}} - \sigma } \right)\left({\frac{{9{{\bar {d}}_j}\alpha _{0}^{2}}}{{8{\omega _j}} - \sigma } \right)<0
53
.

Eq. (53) indicates that the nonlinear term affects the stability of the steady-state solutions. So both the nonlocal effect and the material nonlinearity affect the stability of the solutions. In the response curves in the next section (Fig. 5–7 and Fig. 11–12), the solid line represents the stable solutions and the dashed line represents the unstable solutions.

4. Results And Discussion

It is necessary to point out that nanobeam's mechanical properties' experiments are challenging, and the existing experimental results have significant errors [17, 51]. Molecular dynamics (MD) calculations of SWCNTs show a big gap between the calculated results and the classical models that do not include scale effects or physical nonlinearity [52, 53]. Furthermore, MD calculations confirm that the calculations' results are consistent with the models with the nonlocal effect [9, 31] or physical nonlinearity [16]. The present theories consider nonlocal effects and physical nonlinearity comprehensively, which provides a basis to fit the mechanical parameters of carbon nanotubes through experiments or MD calculations.

This section uses \left({15,15} \right) SWCNTs to demonstrate the differences between the four theories. So the diameter is d=2.034\;\text{n}\text{m}, and the thickness is taken as h=0.34\;\text{n}\text{m}, the other physical and geometrical parameters are [15, 22]: E=1\;\text{T}\text{P}\text{a}, D= - 2\;\text{T}\text{P}\text{a}, m=4.86 \times {10^{ - 15}}\;\text{k}\text{g}{\text{m}^{-1}}, I=1.115\;\text{n}

{\text{m}^4}, A=2.171\;\text{n}{\text{m}^2}, \lambda = - 1.027 \times {10^{ - 18}}\;\text{n}{\text{m}^2}, {\bar {c}_1}={\bar {c}_2}=0.01. As mentioned in the introduction, determining the non-local parameter {e_0} of SWCNTs is an open problem. This problem may come from ambiguous understandings of one-atom-thick nanostructure's mechanical properties [32, 54]. The non-local parameter obtained by atomic calculations has also shown some confusion [17, 31, 55]. However, if the vibration frequency in CNTs is in the terahertz range, a conservative estimate is {e_0}a<2\;\text{n}\text{m} [5, 55]. In the present research, we take the SWCNT's scale coefficient \mu ={e_0}a=1\;\text{n}\text{m}. It is bigger than most values in the existing researches of SWCNTs [5]. Using a big nonlocal coefficient may help compare the material nonlinearity and the non-local effect.

4.1. Hinged-hinged SWCNTs

It can find from Eqs. (40) that the nonlinear parameter is related to the beam length. We first focus the length's effect on {d_1}, as shown in Fig. 2. The figure and Eqs. (40) show that {d_1} in the CNM and the NNM is positive for \left({15,15} \right) SWCNTs. This indicates that the geometrical nonlinear terms, which are induced by finite deformations and the nonlocal effect, produce a hardening effect for the SWCNTs. However, when the material nonlinearity appears in the models (NCM and NNCM), {d_1} will change from positive to negative with the length's decrease, as shown in Fig. 2. This means that the nonlinear terms in Eqs. (39) change from a soft spring to a hard spring. Nonlinear springs significantly influence the nonlinear mechanical properties of macrostructures [35–50].

Here we take l=8\text{n}\text{m} and l=6\text{n}\text{m} as examples to study the differences between four beam theories. Since the nonlinear coefficients in the four models are all greater than zero for l=8\text{n}\text{m}, the SWCNT is a hard spring system ({d_1}>0). However, for l=6\text{n}\text{m}, the models with material nonlinearity (NCM and NNCM) are soft spring systems ({d_1}<0), while other models (CNM and NNM) are still hard spring systems ({d_1}>0). The static load-deformation curves can be obtained from Eq. (41) with j=1, as shown in Fig. 3 and Fig. 4. The two figures show that the softening effect remarkably increases the deformation amplitudes of the static bending. Further, the material nonlinearity may significantly impact the SWCNT's vibrations under the primary resonance, as shown in Fig. 5 to Fig. 7 obtained from Eq. (51) with j=1. For example, four load-response curves at \sigma =10 are significantly different between l=8 and l=6, as shown in Fig. 5 and Fig. (6). The two figures show that the material nonlinearity in short tubes is more prominent than in long tubes. Therefore ignoring the material nonlinearity may lead to evident errors for short SWCNTs, as shown in Fig. 7 and Fig. 8. The material nonlinearity produces the softening effect in the NCM and NNCM for l=6, and the softening effect makes their frequency-response curves deviate to the left. On the contrary, the nonlinear terms in the CNM and the NNM are hard springs. This makes the frequency-response curves are skewed to the right, as shown in Fig. 7. We calculated Eq. (42) numerically through the Runge-Kutta method for \left({l,\sigma ,f} \right)=\left({6,5,5} \right). The results show that ignoring the material nonlinearity may seriously underestimate the vibration amplitudes, as shown in Fig. 8. The numerical calculations also show the perturbation solution's accuracy.

4.2 Simply supported SWCNTs

Here we will demonstrate the tube length's influence on the nonlinear coefficients {d_2} for simply supported SWCNTs, as shown in Fig. 9. It is found in Fig. 9 and Eqs. (40) that the material nonlinearity makes {d_2}<0 for the NCM and NNCM. This indicates that both the non-local effect and the material nonlinearity have a stiffness softening effect on SWCNTs. The softening makes static bending deformations of the NNM and the NNCM significantly larger than these of the CNM and the NNM when the SWCNTs are subjected to big loads, as shown in Fig. 10 obtained by Eq. (41) with j=2. Furthermore, the material nonlinearity more significantly affects the dynamic behaviors of SWCNTs under the primary resonance. For example, the response amplitudes of the NCM and the NNCM have jumps accompanying excitation amplitude's change, while the CNM and NNM do not produce amplitude's jumps for \left({l,\sigma } \right)=\left({6, - 5} \right), as shown in Fig. 11 obtained by Eq. (51) with j=2. Similar to the hinged-hinged beams, the frequency-response curves of the NCM and the NNCM appear maximum vibration amplitudes in \Omega <{\omega _2}. In contrast, the maximum vibration amplitudes of the CNM and the NNM appear in \Omega >{\omega _2}, as shown in Fig. 12 obtained by Eq. (51). The above results indicate that one may obtain incorrect results if the material nonlinearity or nonlocal effects are neglected. We implement numerical calculations of Eq. (42) through the Runge-Kutta method to check the perturbation solutions Eq. (51). The numerical simulations confirm the accuracy of the analytical solutions, as shown in Fig. 13.

5. Conclusions

In the present study, we combine the non-local effect and the material nonlinearity to suggest two new Euler-Bernoulli models for nanobeams. The integral-partial differential equation models the axial extensional effect. Another partial differential equation models the axial inextensional effect. (15,15) SWCNTs are used as examples to research the static bending and the forced vibration for the hinged-hinged and simply supported nanobeams. The results show that the material nonlinearity significantly softens SWCNT's stiffness. Both the material nonlinearity and nonlocal effects significantly impact the mechanical properties of SWCNTs. Noticeable mistakes may appear if one neglects the material nonlinearity or the nonlocal effect.

Declarations

Conflict of interest: The authors declare that they have no conflict of interest.

Data Availability Statements

The datasets generated during and/or analysed during the current study are available from the corresponding author on reasonable request.

Compliance with ethical standards

Acknowledgements:

This work was supported by the National Natural Science Foundation of China (grant no. 11562009 and 12050001).

References

1. Elishakoff, I., Dujat, K., Muscolino, G., et al.: Carbon Nanotubes and Nanosensors: Vibration, Buckling and Balistic Impact. John Wiley & Sons, London (2013)
2. Eichler, A., del Álamo Ruiz, M., Plaza, J.A., et al.: Strong coupling between mechanical modes in a nanotube resonator. *Physical review letters* 109(2), 025503 (2012)
3. Reddy, J.N.: Nonlocal theories for bending, buckling and vibration of beams. *International journal of engineering science* **45(2-8)**, 288-307 (2007);
4. Ghaffari, S.S., Ceballes, S., Abdelkefi, A.: Nonlinear dynamical responses of forced carbon nanotube-based mass sensors under the influence of thermal loadings. Nonlinear Dynamics **100(2)**, 1013-1035 (2020)
5. Rafii-Tabar, H., Ghavanloo, E., Fazelzadeh, S.A.: Nonlocal continuum-based modeling of mechanical characteristics of nanoscopic structures. *Physics Reports* **638**, 1-97 (2016)
6. Peddieson, J., Buchanan, G.R., McNitt, R.P.: Application of nonlocal continuum models to nanotechnology. *International journal of engineering science* **41(3-5)**, 305-312 (2003)
7. Eringen, A.C: On differential equations of nonlocal elasticity and solutions of screw dislocation and surface waves. *J Appl Phys* **54**, 4703–4710 (1983)
8. Lee, H., Hsu, J.C., Chang, W.J.: Frequency Shift of Carbon-Nanotube-Based Mass Sensor Using Nonlocal Elasticity Theory. *Nanoscale Res Lett* **5**, 1774 (2010)
9. Askes, H., Aifantis, E.C.: Gradient elasticity in statics and dynamics: an overview of formulations, length scale identification procedures, finite element implementations and new results. *International Journal of Solids and Structures.* **48(13)**, 1962-1990 (2011)
10. Güven, U.: Transverse vibrations of single-walled carbon nanotubes with initial stress under magnetic field. Composite Structures **114**, 92-98 (2014)
11. Cordero, N.M., Forest, S., Busso, E.P.: Second strain gradient elasticity of nano-objects. *Journal of the Mechanics and Physics of Solids* **97**, 92-124 (2016)
12. Colombo, L., Giordano, S.: Nonlinear elasticity in nanostructured materials. *Reports on Progress in Physics* **74(11)**, 116501 (2011)
13. Chen, H., Zarkevich, N.A., Levitas, V.I., et al.: Fifth-degree elastic energy for predictive continuum stress–strain relations and elastic instabilities under large strain and complex loading in silicon. *npj Computational Materials* **6(1)**, 1-8 (2020)
14. Cadelano, E., Palla, P.L., Giordano, S., Colombo, L.: Nonlinear elasticity of monolayer graphene. *Physical review letters* **102(23)**, 235502 (2009)

15. Lee, C., Wei, X., Kysar, J.W., Hone, J.: Measurement of the elastic properties and intrinsic strength of monolayer graphene. *Science* **321(5887)**, 385-388 (2008)
16. Wang, Y., Fang, D., Soh, A.K., Liu, B.: A molecular mechanics approach for analyzing tensile nonlinear deformation behavior of single-walled carbon nanotubes. *Acta Mechanica Sinica* **23(6),** 663-671 (2007)
17. Chandel, V.S., Wang, G., Talha, M.: Advances in modelling and analysis of nano structures: a review. *Nanotechnology Reviews* **9(1)**, 230-258 (2020)
18. Huang, K., Zhang, S., Li, J., Li, Z.: Nonlocal nonlinear model of Bernoulli–Euler nanobeam with small initial curvature and its application to single-walled carbon nanotubes. *Microsystem Technologies* 25(11): 4303-4310. (2019)
19. Jin L, Li L.: Nonlinear Dynamics of Silicon Nanowire Resonator Considering Nonlocal Effect. *Nanoscale Res Lett* **12**, 331 (2017)
20. Ansari, R., Ramezannezhad, H., Gholami, R.: Nonlocal beam theory for nonlinear vibrations of embedded multiwalled carbon nanotubes in thermal environment. *Nonlinear Dynamics* **67(3)**, 2241-2254 (2012)
21. Li, L., Hu, Y.: Nonlinear bending and free vibration analyses of nonlocal strain gradient beams made of functionally graded material. *International Journal of Engineering Science* **107**, 77-97 (2016)
22. Huang, K., Cai, X., Wang, M.: Bernoulli-Euler beam theory of single-walled carbon nanotubes based on nonlinear stress-strain relationship. *Materials Research Express* **7(12)**, 125003 (2020)
23. Guo, W., Guo, Y.: Giant axial electrostrictive deformation in carbon nanotubes. *Physical review letters* **91(11)**, 115501 (2003)
24. Huang, K., Yao, J.: Beam Theory of Thermal–Electro-Mechanical Coupling for Single-Wall Carbon Nanotubes. *Nanomaterials* **11(4)**, 923 (2021)
25. Askes, H., Aifantis, E.C.: Gradient elasticity and flexural wave dispersion in carbon nanotubes. *Physical Review B* **80(19)**, 195412 (2009)
26. Lim, C.W., Zhang, G., Reddy, J.N.: A higher-order nonlocal elasticity and strain gradient theory and its applications in wave propagation. *Journal of the Mechanics and Physics of Solids* **78**, 298-313 (2015)
27. Wang, G.F., Feng, X.Q.: Effects of surface elasticity and residual surface tension on the natural frequency of microbeams. *Applied physics letters* **90(23)**, 231904 (2007)
28. Pradhan, S.C., Phadikar, J.K.: Small scale effect on vibration of embedded multilayered graphene sheets based on nonlocal continuum models. *Physics letters A* **373(11)**, 1062-1069 (2009)
29. Jalaei, M.H., Arani, A.G., Tourang, H.: On the dynamic stability of viscoelastic graphene sheets. *International Journal of Engineering Science* **132**, 16-29 (2018)
30. Zhao, J., Guo, X., Lu, L.: Small size effect on the wrinkling hierarchy in constrained monolayer graphene. *International Journal of Engineering Science* **131**, 19-25 (2018)

31. Duan, W.H., Wang, C.M., Zhang, Y.Y.: Calibration of nonlocal scaling effect parameter for free vibration of carbon nanotubes by molecular dynamics. *Journal of applied physics* **101(2)**, 024305 (2007)
32. Huang, K., Yin, Y., Qu, B.: Tight-binding theory of graphene mechanical properties. *Microsyst Technol*. **27,** 3851–3858 (2021)
33. Huang, K., Yin, Y., Wu, J.Y.: A nonlinear plate theory for the monolayer graphene Acta Phys. Sin. **63**, 156201 (2014)
34. Washizu, K.: Variational Methods in Elasticity and Plasticity, Pergamon, Oxford (1975)
35. Lacarbonara, W.: Nonlinear Structural Mechanics Nonlinear Structural Mechanics, Theory, Dynamical Phenomena and Modeling. Springer, Berlin (2013)
36. Nayfeh, A.H., Mook, D.T.: Nonlinear Oscillations. Wiley, New York (2008)
37. Nayfeh, A. H., Pai, P. F.: *Linear and Nonlinear Structural Mechanics*. John Wiley & Sons, New York, 2008
38. Nayfeh, A. H., Nayfeh, J. F., Mook, D. T.: On methods for continuous systems with quadratic and cubic nonlinearities. Nonlinear Dynamics **3(2)**, 145-162 (1992)
39. Emam, S. A., Nayfeh, A. H.: Non-linear response of buckled beams to 1: 1 and 3: 1 internal resonances. International Journal of Non-Linear Mechanics 52, 12-25 (2013)
40. Arafat, H. N., Nayfeh, A. H.: Non-linear responses of suspended cables to primary resonance excitations. Journal of Sound and Vibration **266(2)**, 325-354 (2003)
41. Luongo, A., Egidio, A. D.: Bifurcation equations through multiple-scales analysis for a continuous model of a planar beam. Nonlinear Dynamics **41(1)**, 171-190 (2005)
42. Di Egidio, A., Luongo, A., Paolone, A.: Linear and non-linear interactions between static and dynamic bifurcations of damped planar beams. International Journal of Non-Linear Mechanics **42(1)**, 88-98 (2007)
43. Lacarbonara, W., Yabuno, H.: Refined models of elastic beams undergoing large in-plane motions: theory and experiment. International Journal of Solids and Structures **43(17)**, 5066-5084 (2006)
44. Lacarbonara, W., Rega, G., Nayfeh, A. H.: Resonant non-linear normal modes. Part I: analytical treatment for structural one-dimensional systems. International Journal of Non-Linear Mechanics **38(6)**, 851-872 (2003)
45. Lacarbonara, W.: Direct treatment and discretizations of non-linear spatially continuous systems. Journal of Sound and Vibration **221(5)**, 849-866 (1999)
46. Rega, G., Lacarbonara, W., Nayfeh, A. H., Chin, C.M.: Multiple resonances in suspended cables: direct versus reduced-order models. International Journal of Non-Linear Mechanics **34(5)**, 901-924 (1999)
47. Luongo, A., Paolone, A.: On the reconstitution problem in the multiple time-scale method. *Nonlinear Dynamics* **19(2)**, 135-158 (1999)
48. Huang, K., Feng, Q., Qu, B.: Bending aeroelastic instability of the structure of suspended cable-stayed beam. *Nonlinear Dynamics* **87(4)**, 2765-2778 (2017)

49. Di Nino, S., Luongo, A.: Nonlinear aeroelastic behavior of a base-isolated beam under steady wind flow. *International Journal of Non-Linear Mechanics* **119**, 103340 (2020)
50. Arena, A., Lacarbonara, W.: Piezoelectrically induced nonlinear resonances for dynamic morphing of lightweight panels. Journal of Sound and Vibration **498**, 115951 (2021)
51. Kis, A., Zettl, A.: Nanomechanics of carbon nanotubes. Philosophical Transactions of the Royal Society A: Mathematical, Physical and Engineering Sciences **366(1870)**, 1591-1611 (2008)
52. Genoese, A., Genoese, A., Salerno, G.: Buckling and post-buckling analysis of single wall carbon nanotubes using molecular mechanics. Applied Mathematical Modelling **83**, 777-800 (2020)
53. Fang, C., Kumar, A., Mukherjee, S.: Finite element analysis of single-walled carbon nanotubes based on a rod model including in-plane cross-sectional deformation. International Journal of Solids and Structures **50(1)**, 49-56 (2013)
54. Huang, K., Wu, J., Yin, Y.: An Atomistic-Based Nonlinear Plate Theory for Hexagonal Boron Nitride. *Nanomaterials* **11**, 3113 (2021)
55. Wang, Q., Wang, C.M.: The constitutive relation and small scale parameter of nonlocal continuum mechanics for modelling carbon nanotubes. *Nanotechnology***18(7)**, 075702 (2007)

Figures

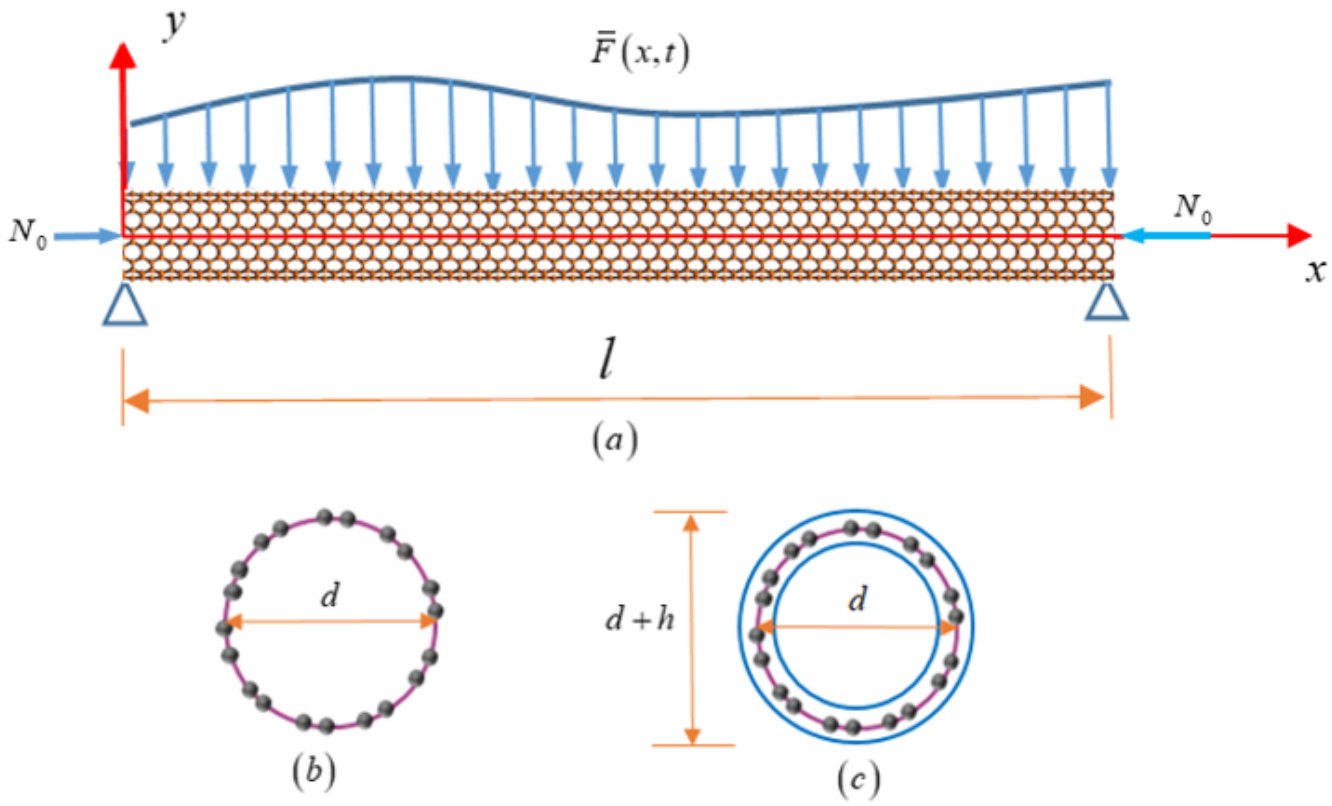

Figure 1

Schematic configuration of a SWCNT, (a) Front elevation, (b) Plan, (c) Equivalent cross-section

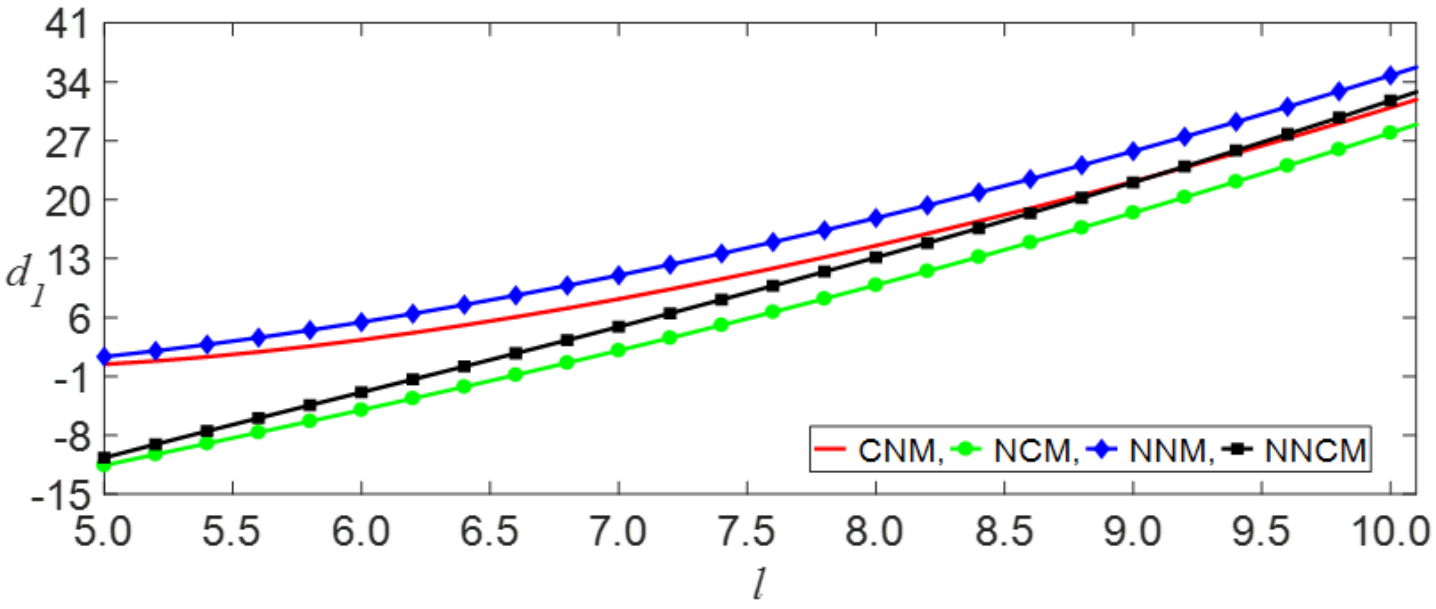

Fig. 2. Nonlinear coefficients d_1 as functions of hinged-hinged beam lengths l.

Figure 2

See image above for figure legend

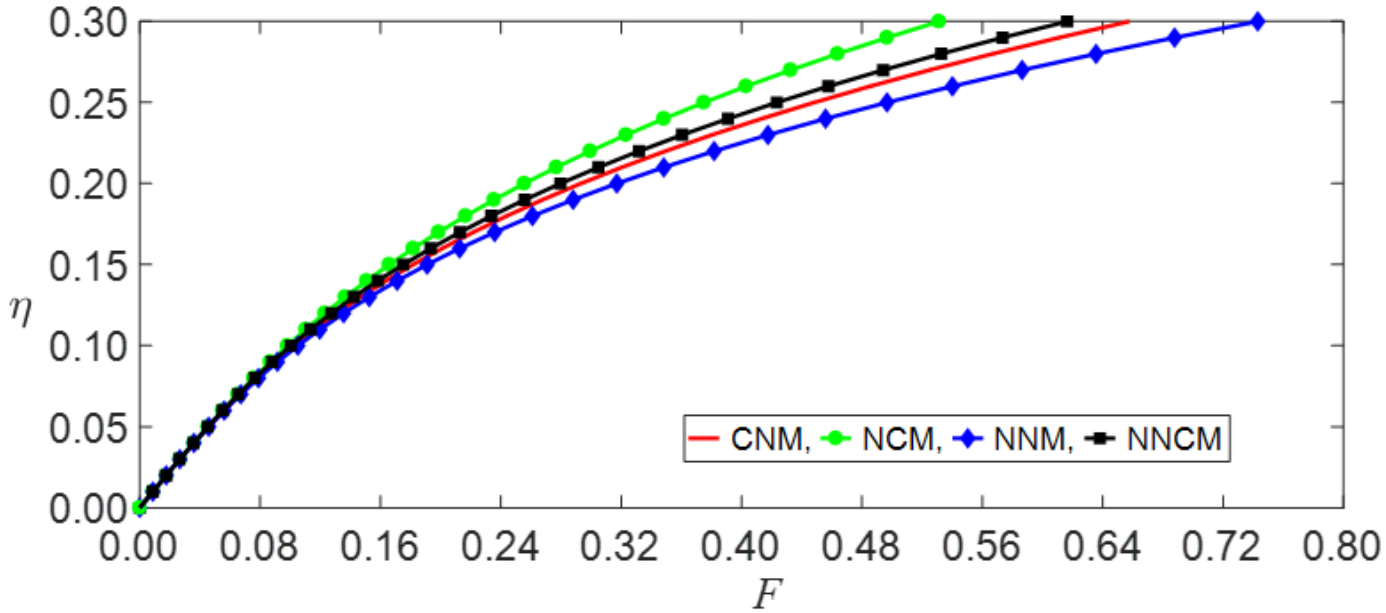

Fig. 3. Static deformations as functions of loads for hinged-hinged beams at $l = 8$.

Figure 3

See image above for figure legend

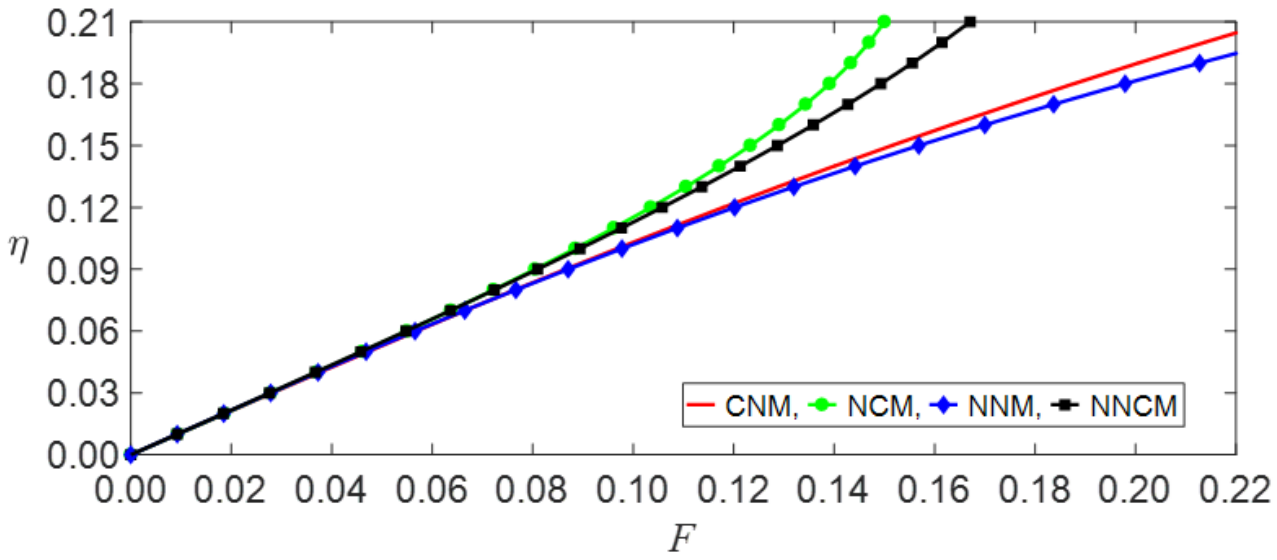

Fig. 4. Static deformations as functions of loads for hinged-hinged beams at $l = 6$.

Figure 4

See image above for figure legend

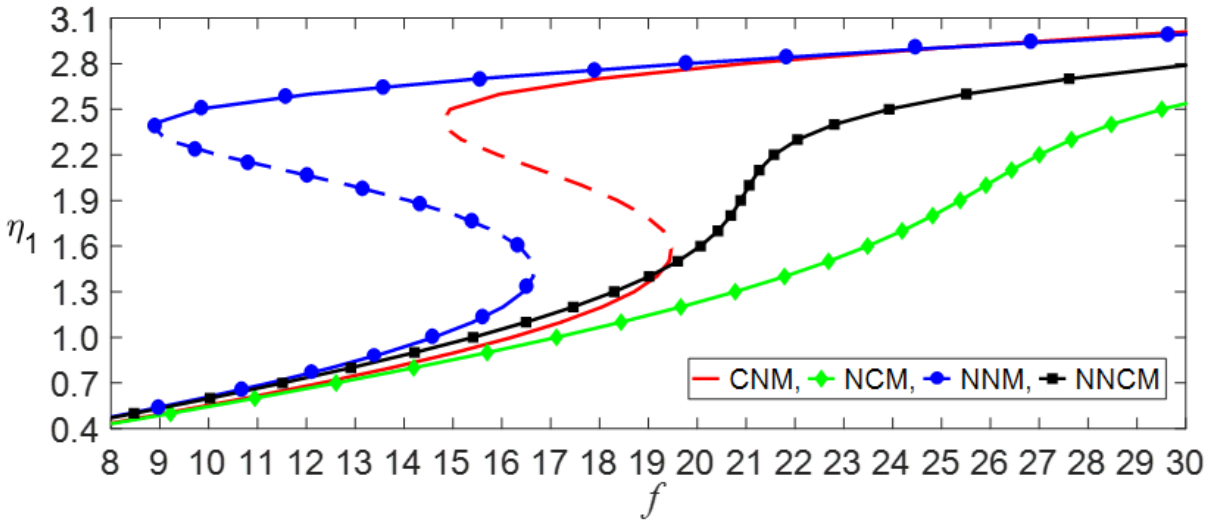

Fig. 5. Amplitudes of response as functions of the amplitudes of loads for hinged-hinged beams at $(l, \sigma) = (8, 10)$.

Figure 5

See image above for figure legend

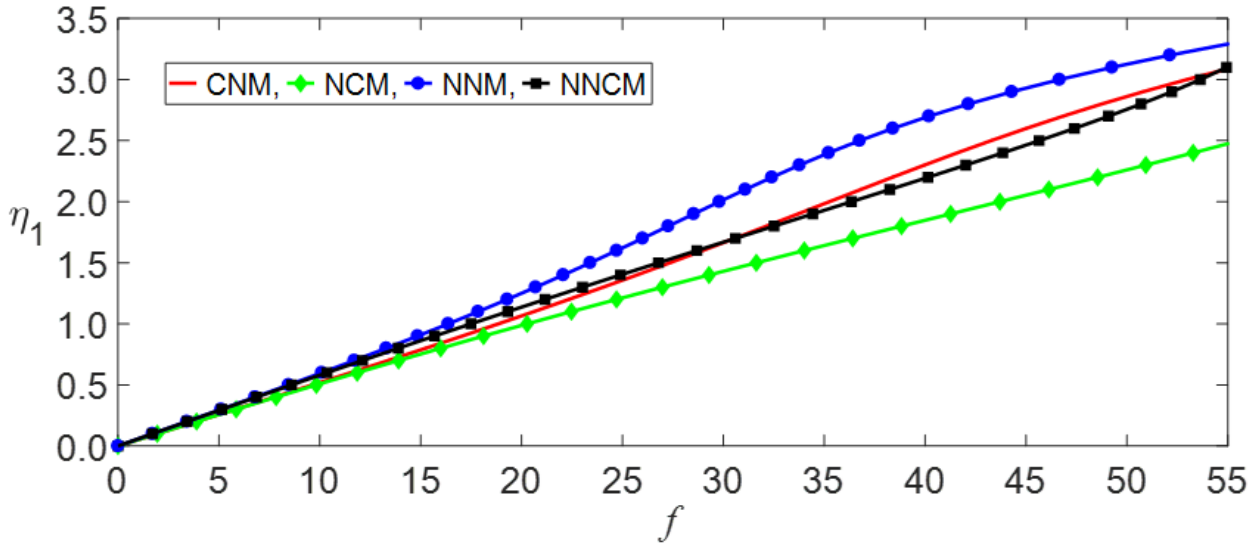

Fig. 6. Amplitudes of response as functions of the amplitudes of loads for hinged-hinged beams at $(l,\sigma)=(6,10)$.

Figure 6

See image above for figure legend

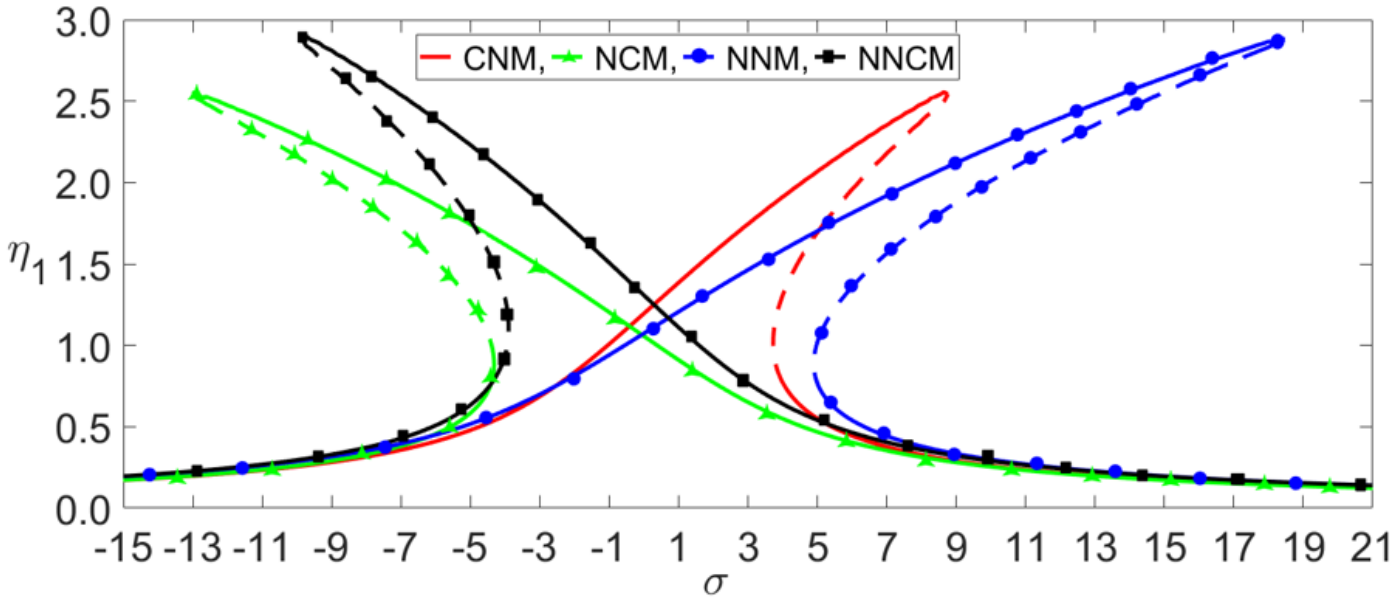

Fig. 7. Frequency-response curves for hinged-hinged beams at $(l,f)=(6,5)$

Figure 7

See image above for figure legend

Figure 8

See image above for figure legend

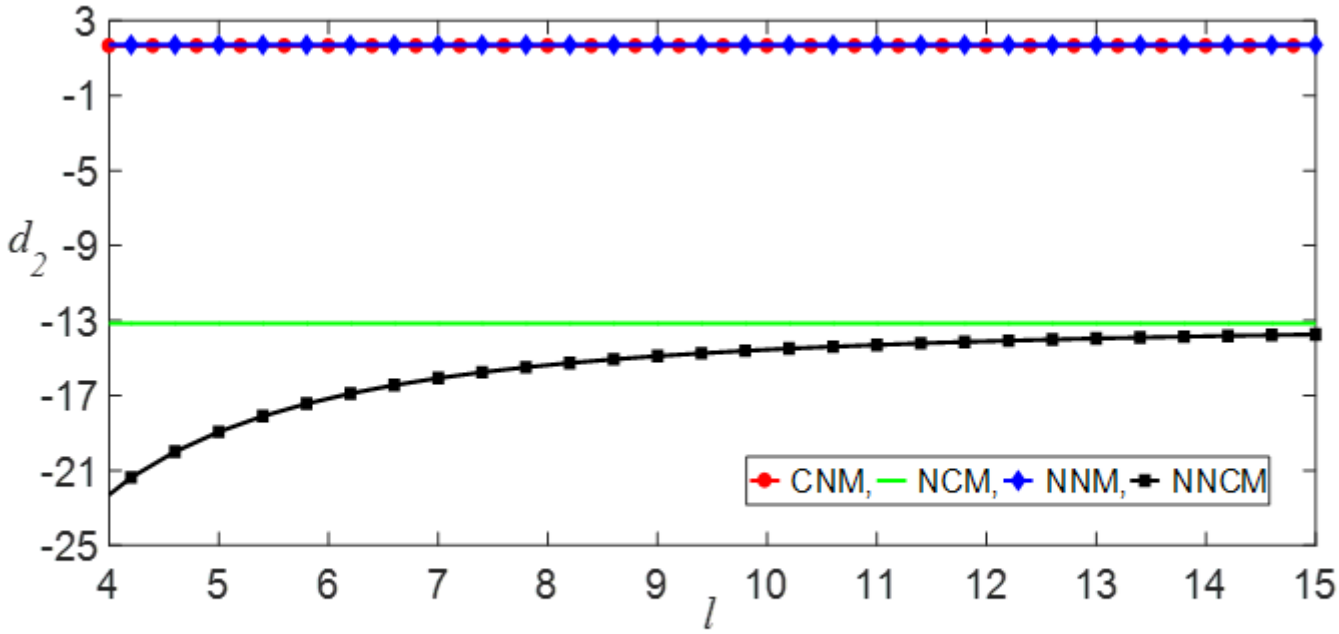

Fig. 9. Nonlinear coefficients d_2 as functions of simply supported beam lengths l.

Figure 9

See image above for figure legend

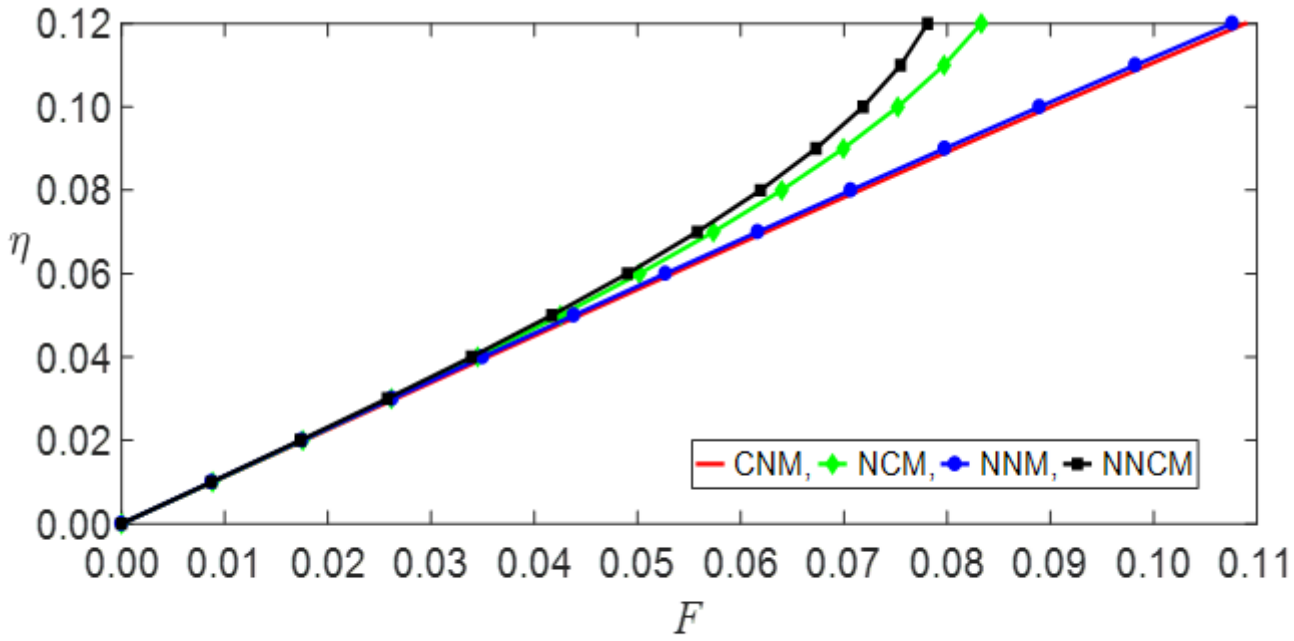

Fig. 10. Static deformations as functions of loads for simply supported beams at $l=8$.

Figure 10

See image above for figure legend

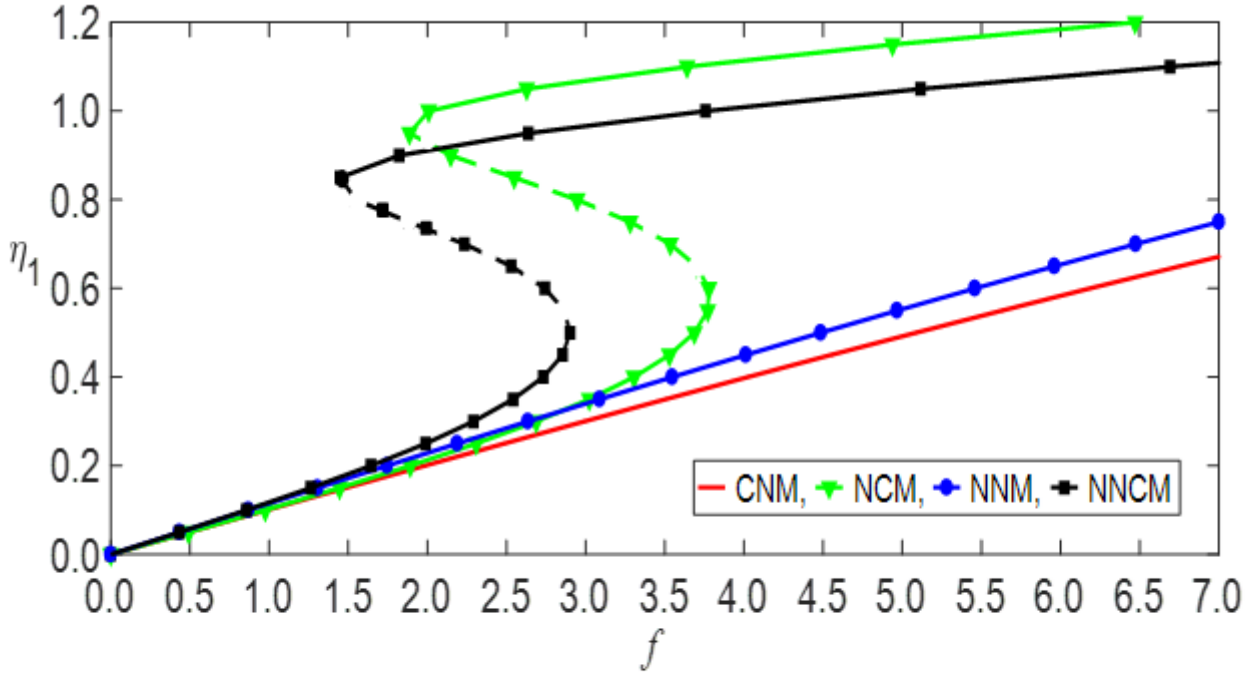

Fig. 11. Amplitudes of response as functions of the amplitudes of loads for simply supported beams at $(l,\sigma)=(6,-5)$.

Figure 11

See image above for figure legend

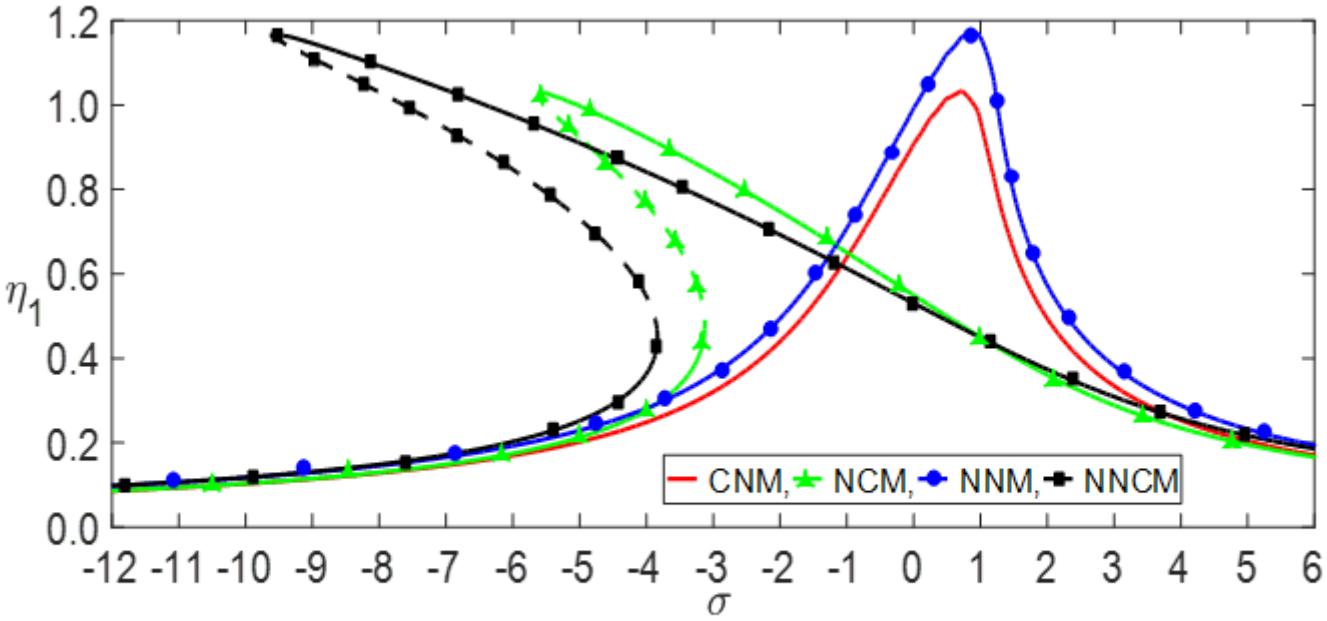

Fig. 12. Frequency-response curves for simply supported beams at $(l, f) = (6, 2)$

Figure 12

See image above for figure legend

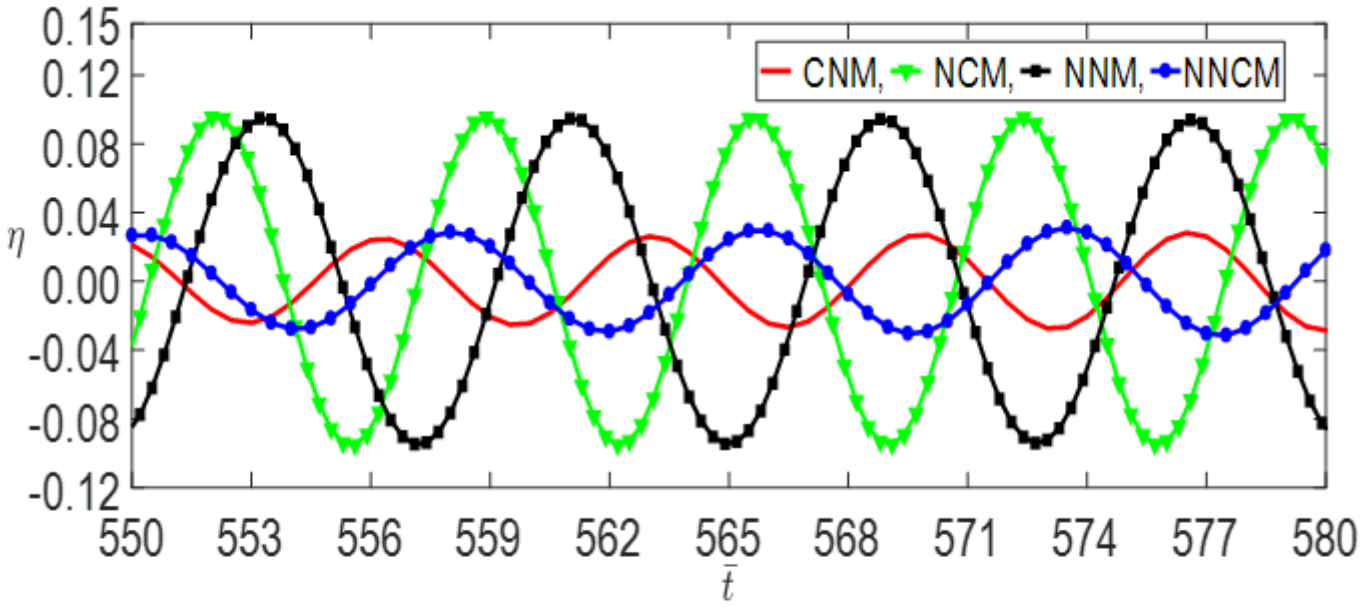

Fig. 13. Time series of hinged-hinged beams for $(l, \sigma, f) = (6, -4, 2)$ at an initial value

$$(\eta, \dot{\eta}) = (0.1, 0)$$

Figure 13

See image above for figure legend